

# Degradation of the textile dyes Basic yellow 28 and Reactive black 5 using diamond and metal alloys electrodes

M. Cerón-Rivera<sup>a</sup>, M.M. Dávila-Jiménez<sup>b</sup>, M.P. Elizalde-González<sup>a,\*</sup>

<sup>a</sup> Centro de Química, Instituto de Ciencias, Universidad Autónoma de Puebla, Apdo. Postal J-55, Puebla, Pue. 72571, Mexico

<sup>b</sup> Facultad de Ciencias Químicas, Universidad Autónoma de Puebla, Apdo. Postal J-55, Puebla, Pue. 72571, Mexico

Received 15 July 2003; received in revised form 29 October 2003; accepted 29 October 2003

## Abstract

Basic yellow 28 (SLY) and Reactive black 5 (CBWB), which are respectively methine and sulfoazo textile dyes were individually exposed to electrochemical treatment using diamond-, aluminium-, copper- and iron–zinc alloy electrodes. The generated current was registered with time during electrolysis of the dye solutions and the color variation and the formation of degradation products were followed using HPLC with diode array detection. Four different electrodic materials were tested by applying different potentials in the range  $-1.0$  to  $-2.5$  V and presented 95% color removal and COD removal of up to 65–67% in the case of CBWB dye solution treated with the copper and iron electrodes. Efficiency was enhanced with stirring and flow in relation to the stationary regime. The kinetic parameter reaction rate was used to establish the effect of flow, potential, electrode nature and pH. The formation and characterization of the precipitate formed under certain conditions is reported and discussed.

© 2003 Elsevier Ltd. All rights reserved.

**Keywords:** Dyes; Electroreduction; Diamond; Aluminium electrode; Copper electrode; Iron electrode

## 1. Introduction

Textile industry is one of the most polluting sectors when discharge volumes and effluent composition are considered. The treatment of its wastewater is commonly carried out using biological (Delée et al., 1998) and physico-chemical methods (Vandevivere et al., 1998). However, many of the commercially used dyes are resistant to biodegradation. As a result, coagulation (Vandevivere et al., 1998), coagulation–electrooxidation (Xiong et al., 2001), adsorption (Morais et al., 1999), electrolysis (Dávila-Jiménez et al., 2000), photolysis (Ince, 1999) and ozonation are promising in terms of

performance, while the economic aspect has become the most challenging problem. At this time small scale oxidizing methods use Fenton's reagent (Powell et al., 1994), which has lower costs in comparison with ozone process in dye liquors treatment (Gregor, 1994). The oxidizing effect of the Corona discharge is also known and it has been reported by Goheen et al. (1994) as an effective method to bleach organic dyes using a stainless steel electrode.

Recently new results of Yang et al. (2000) on the color removal in dye wastewater were reported by applying electrogenerated hypochlorite ions and (Ru + Pt)<sub>x</sub> binary electrodes. However, the removal of dyes from wastewater in an economic way by using electrochemical methods and low-cost electrodes remains a major concern. Therefore there is a growing interest in using easily available materials, the so-called sacrificial electrodes. Carbon (McClung and Lemley,

\* Corresponding author.

E-mail address: melizald@siu.buap.mx (M.P. Elizalde-González).

1994; Sheng and Peng, 1994; Xiong et al., 2001), Ti/Pt (Vlyssides et al., 2000), aluminium (Kobyta et al., 2003) and iron (DeFazio and Lemley, 1999) electrodes have been tested. Performance of a carbon fiber electrode (Jia et al., 1999) was comparable, for example, with that of the Fenton's reagent. Cu, Pt, Ni, Ti and diamond electrodes were useful (Dávila-Jiménez et al., 2000) in studying the decomposition of textile dyes by means of high performance liquid chromatography (HPLC). However, maximum efficiency reached in that work was 70% due probably to poisoning of those solid electrodes. Evidently sponge and screen electrodes should present different behavior and offer better mass transfer operating variables. The enhancement of the mass transfer avoids saturation of the electrode surface and in consequence, improves the efficiency of electrochemical reactors as demonstrated by Sedahmed et al. (1986) for example, in stirred systems and with air flow (Xiong et al., 2001). Care must be taken in considering reports on degradation of dyes, where the process has been monitored and has been erroneously called by the authors "dynamic electrolysis" (Shen et al., 2001).

Commonly the electrochemical technology to remove color uses steel electrodes to generate ferrous hydroxide and ferric oxyhydroxide. The treated water and the newly forming solids pass to a clarifier to subsequently handling. To reduce solids generation the two most important factors are pH and solubility both of electrode ions and precipitates. Therefore, the performance of non-conventional electrodes with diverse composition and the impact of the metal solubility can also be explored.

Generally textile effluents have a complex and variable composition, but the use of a simulated waste by means of an artificial aqueous solution facilitates the assessment of a treatment process for emerging technology. Our work was focused on testing several

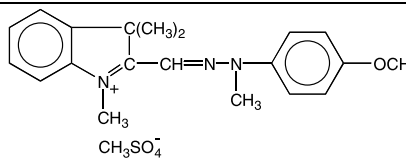
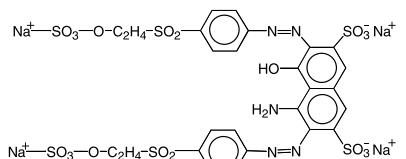
electrode materials for the electrochemical treatment of selected textile dyes under dynamic conditions with mass transfer. Previous studies had used in situ colorimetric measurements, or parameters like chemical oxygen demand (COD) and total organic carbon (TOC), for determining the dyes removal from model solutions. This investigation presents the use of metal alloys electrodes, new conditions for the electrochemical treatment and the analysis of the treated artificial solution by HPLC to follow the quenching of the color and the formation of uncolored breakdown products.

## 2. Materials and methods

### 2.1. Chemicals

Dyes listed in Table 1 were chosen because of their extended regional use. Sandocryl gold yellow (Basic yellow 28) was Clariant product number 14277. Navy blue Cibacron WB dye is produced by Ciba. They were used as received and the relative content in the samples determined by HPLC at 220 nm was 89–90%. Other minor components (10–11%) could correspond to dye-stuff intermediates or compounds, which served as start materials in the dye synthesis. Dyes solutions with concentration 100 mg l<sup>-1</sup> were prepared in purified water obtained from a Milli-Q reagent grade water system. The same was used in the chromatographic analysis together with Methanol HPLC grade. Phosphates buffer was prepared from reagent grade salts from J.T. Baker Chemical (Phillisburg, NJ, USA), with a ionic strength  $\mu = 1.54$ . The electrodic materials designated as Al99, Cu74 and Fe52 were used. Their respective metal content was 99% aluminium, 74% copper and 52% iron as determined by X-ray fluorescence spectroscopy. The complementary second component was Zn and trace

Table 1  
Textile dyes and name abbreviations used in this study

Code	Structural formulae	Commercial name	Color index	$\lambda_{\max}$ (nm)	M
SLY		Gold Yellow Sandocryl	Basic yellow 28	450	433
CBWB		Navy blue Cibacron WB	Reactive black 5	600	991

metals in definite amounts were: Cr 0.07%, Mn 0.02%, Fe 0.08%, Cu 0.01% in A199, Cr 0.01%, Mn 0.01%, Fe 0.4% in Cu74 and Cr 0.1%, Mn 0.3%, Cu 0.2%, Mo 0.02% in Fe52.

## 2.2. Apparatus

Electrodes analysis was carried out by X-ray fluorescence spectroscopy (Spectrace Instruments) at the following tube voltage, tube current and atmosphere, respectively: 6 kV, 0.10 mA, vacuum for A199; 30 kV, 0.20 mA, air for Cu74 and Fe52. Electrolysis was carried out at potentials varying from  $-1.0$  to  $-2.5$  V using a home made potentiostat–galvanostat registered with the Puebla (Mexico) and Lodz (Poland) universities acronyms, as UAP/LODZ and the working electrodes were diamond and those indicated in the previous section. Geometric area was  $3\text{ cm}^2$  for diamond and  $18\text{ cm}^2$  for the metallic electrodes. The diamond electrode consisted of a Ti-sheet coated with diamond with a  $0.1\text{--}1\text{ }\mu\text{m}$  thickness and was purchased from DiaChem®-Electrodes. The auxiliary electrode consisted of a nickel bar ( $>30\text{ cm}^2$ ) and in all cases a saturated Calomel reference electrode was used. The cell (100 ml) consisted of a cylindrical, jacketed reaction kettle with one upper and one lower tubulation for pump tubing. A ground seal three-necked cover enabled vertical positioning of the electrodes. A peristaltic pump Spetec Perimax 12 was utilized to produce a continuous circulation into the electrolysis cell. Before electrolysis the system was kept at open circuit during 5 min. Initial solutions were analyzed utilizing a Beckman DU 7500 spectrophotometer. The chromatographic system consisted of a Beckman Gold system with diode array detector. The chromatographic separations were performed on Beckman Octyl column (15 cm long with 4.6 mm ID). All were stainless steel columns with  $5\text{-}\mu\text{m}$  packing. Mobile phase composition was 20% methanol–aqueous buffer solution  $\text{KH}_2\text{PO}_4 \cdot \text{Na}_2\text{HPO}_4$  with pH 5. Flow rate was  $0.8\text{ ml min}^{-1}$  and analysis was performed at ambient temperature. The sludge characterization was performed by using a Shimadzu model XD 5A X-ray diffractometer with a Cu-K $\alpha$  X-ray source ( $1.5418\text{ \AA}$ ) at 30 mA and 30 kV. The scan speed was set at  $0.5^\circ\text{ min}^{-1}$ . The angular range was from  $20^\circ$  to  $100^\circ$ . The measurement temperature was  $30\text{ }^\circ\text{C} \pm 1$ . A Nicolet Magna FT-IR-750 spectroscopy apparatus was employed to determine the presence of functional groups and a Beckman DU 7500 spectrophotometer was used to analyze the sludge leachate.

## 2.3. Procedures

Prior to each electrolysis UV–VIS spectra of dye solutions were obtained to establish their maximum absorbance wavelength and every dyestuff was chro-

matographed individually at two detection wavelengths: at 450 nm for the methine class Gold yellow Sandocryl (SLY) dye and at 590 for the disazo class Navy blue Cibacron WB (CBWB) dye. The second detection channel was set at 220 nm wavelength for every dye to determine dye purity and the formation of degradation products, which did not exhibit color.

Batch electrochemical treatments of 50 ml solution were carried out in the glass cell described above in the presence of oxygen in phosphates buffer solution (pH 7). In order to obtain reproducible results, electrodes were degreased in  $\text{CCl}_4$  during 3 min in an ultrasonic bath, rinsed with acetone and then water before being placed in the cell. The anode was sanded and washed with concentrated  $\text{H}_2\text{SO}_4$  between different experiments. Experiments were carried out under stationary regime and with flow allowing the solution to circulate through the cell with the help of a peristaltic pump. The flow velocity could be ranged from 1 to  $5\text{ ml min}^{-1}$ , it was regulated by the pump and measured by means of a calibrated rotameter. All electrolysis were carried out at  $25\text{ }^\circ\text{C}$  in triplicate and resulting graphs present mean values.

Batch solutions of dyes dissolved in phosphates buffer solution, were chromatographed before and after electrochemical treatment. As control test each not treated solution was analyzed periodically. Maximum variation of the dye concentration was 6%. Under potentiostatic conditions curves current vs. time were registered and aliquots were taken from the batch solution at determined time intervals for HPLC analysis. Aliquots were collected in polycarbonate or Teflon jars and analyzed immediately. From the following calibration curves:  $C(\text{CBWB}) = A_{\text{peak}}/0.2366$  ( $R^2 = 0.9981$ ) and  $C(\text{SLY}) = A_{\text{peak}}/0.1396$  ( $R^2 = 0.9975$ ) the residual dye concentration in  $\text{mg l}^{-1}$  was calculated. COD values were obtained photometrically by the test method B of the ASTM (2003).

## 3. Results and discussion

### 3.1. Diamond electrode

Diamond electrode is rapidly becoming popular and was proposed by Van Hege et al. (2002) for the treatment of retentates of reverse osmosis during electrochemical oxidation. Adsorption has been recognized by Wilcock et al. (1996) as a promoting phenomenon for removal of contaminants via electrochemical processing. However, diamond electrodes (Dávila-Jiménez et al., 2000) and also Cu, Pt, Ni and Ti solid electrodes suffered deactivation after prolonged work caused as it could be demonstrated (Dávila-Jiménez et al., 2000), by the adsorption of the products formed during the electrochemical treatment of dyes. On the other hand,

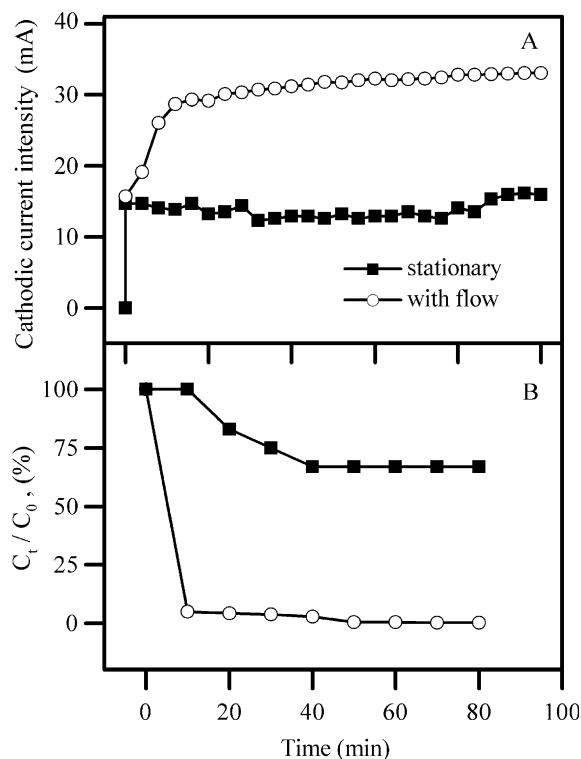


Fig. 1. Current (A) and dye concentration decay (B) curves of Sandocryl yellow during electrochemical treatment at  $-2.5$  V and pH 7 using diamond electrode in stationary regime (■) and with flow (○) at velocity  $3 \text{ ml min}^{-1}$ .

Sedahmed et al. (1986) demonstrated that stirring by gas sparging enhanced efficiency of electrochemical reactors and in full-scale systems wastewater flows through the cell gaps. Since hydrogen evolution already produced gas sparging and to avoid excessive adsorption, we decided to examine the effect of flow on the efficiency of the diamond electrode. Current and concentration decay curves of SLY under different regimes are presented in Fig. 1. Typical polarization curves with well-defined limiting current plateaux were obtained (Fig. 1A). It can be appreciated that the plateau level was reached at lower current value in the stationary regime system in comparison with the dynamic regime and that decolorisation occurred readily and efficiently in the flow

system as it is shown in Fig. 1B. The rate constants shown in Table 2 demonstrate that degradation on the diamond electrode occurred more than 75 times faster under the dynamic regime than under the stationary regime.

### 3.2. Aluminium, copper and iron electrodes

Under the above conditions, the diamond electrode improved its efficiency in dye removal when a dynamic regime was applied. For the electrodes consisting of a metal alloy mesh: Al99, Cu74 and Fe52 we performed electroreduction of the CBWB dye in the flow velocity range  $1\text{--}10 \text{ ml min}^{-1}$ . In this communication results with flow yielding the best experimental conditions, at flow rate  $3 \text{ ml min}^{-1}$  are presented. When considering the energy consumed by the circulating system as a function of flow, low flow rates are a favorable economic factor. A second economic aspect is the energetic cost. So we studied in detail the effect of the applied potential value on the color diminution. Fig. 2A presents this result in the case of the CBWB dye at the Fe52 electrode, where it can be appreciated that at potential  $-1.0$  V slight color removal (14%) was reached after 40 min treatment, while at potential equal or more negative than  $-1.5$  V almost total color removal was achieved. When we examined the  $\log C_t/C_0$  vs.  $t$  curves we obtained from the slopes, that the rate constants (Table 2) of the processes was practically the same starting at  $-1.5$  V and that the difference in the remaining dye concentration was 2%. The experiments reported below correspond to electrolysis performed at potential value  $-2.5$  V and pH 7. Fig. 2B presents the curves for the electrolysis of the CBWB dye by using Al99, Cu74 and Fe52 electrodes. During treatment in all cases, cathodic current intensity increased with time as it was also observed for diamond (Fig. 1A). We found from the rate constants presented in Table 2 that the degradation took place 1.5 times faster on Al99 than on Cu74 and Fe52. Efficiency in terms of the time necessary to descend 50% of the dye concentration ( $t_{50\%}$ ) during electrochemical treatment together with the COD value at the end of the 40 min treatment can be used to compare electrodes performance. Table 3 presents the results of the degradation of the CBWB dye by using four electrodes under dynamic regime with flow velocity  $3 \text{ ml min}^{-1}$ . The final dye concentration

Table 2

Rate constant  $k$  calculated from the linear plot of  $\log(C_t/C_0)$  versus  $t$  in different experiments

$k$ ( $\text{h}^{-1}$ ) for SLY		$k$ ( $\text{h}^{-1}$ ) for CBWB with stirring at $3 \text{ ml min}^{-1}$							
Diamond electrode at pH 7 and $-2.5$ V		Fe52 electrode at pH 7 varying potential				Electrodes at pH 7 and $-2.5$ V		Fe52 electrode at $-2.5$ V varying pH	
Static	With stirring	$-1.0$ V	$-1.5$ V	$-2.0$ V	$-2.5$ V	Al99	Cu74	pH 7	pH 5.5
0.1	7.7	0.1	1.7	1.8	2.0	2.9	2.2	1.8	7.4

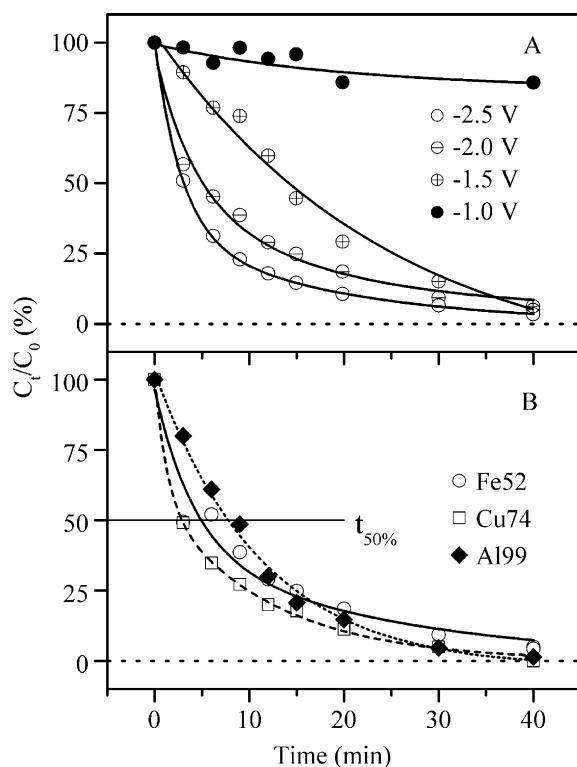


Fig. 2. Cibacron WB concentration decay curves using electrode Fe52 at different potentials (A) and using different electrodes at  $-2.5$  V (B) with flow at  $3 \text{ ml min}^{-1}$ .

after treatment with all three different electrodes differ slightly, nevertheless color disappearance related to concentration diminution of the dye as original molecule, does not mean complete degradation neither complete removal of pollutants in water. Values of COD indicating the removal degree for the studied dyes treated during 40 min with different electrodes are also gathered in Table 3, except for the diamond electrode. The COD initial values for the CBWB dye solutions

Table 3

Electrodes efficiency and pH in the electroreduction of the disazo dye CBWB

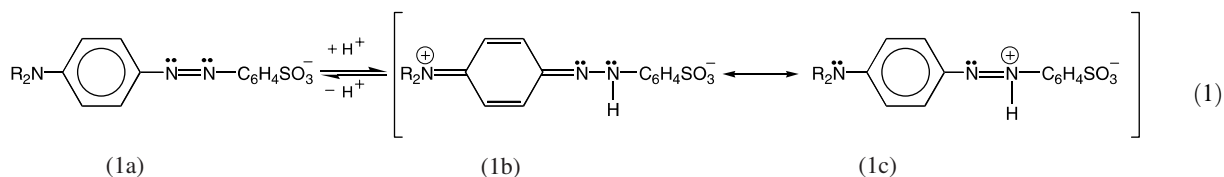
Electrode	Initial pH	$t_{50\%}$ (min)	COD removal efficiency after 40 min electrolysis (%)
Diamond	7	25	
Al99		8	50
Cu74		3	67
Fe52		5	65
Fe52	5.5	3	69

Electrochemical treatment at  $-2.5$  V under dynamic regime with flow at  $3 \text{ ml min}^{-1}$ .

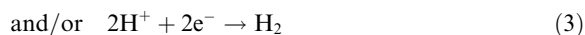
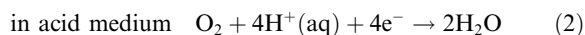
with concentration  $100 \text{ mg l}^{-1}$  was  $615 \text{ mg l}^{-1}$ . The Al99 aluminium electrode consisting of 99% aluminium removed faster but only 50% of the disazo CBWB dye in terms of COD, while the Cu74 and Fe52 electrodes removed 65–69% of the COD, which corresponded to a residual COD value of  $203\text{--}215 \text{ mg l}^{-1}$ , that is within the World Health Organization's (WHO's) allowed maximum level ( $200\text{--}240 \text{ mg l}^{-1}$ ). When watching both at the chemistry of the dye and at its adsorption on the aluminium oxyhydroxide matrix (Wilcock et al., 1996) it could be speculated that a "pure" (99% Al) electrode could yield the best removal efficiency. In our laboratory COD removal was 81–85% for the Mariposa Blue dye with a structure different to that of the CWBW dye by using all the three electrodes Al99, Cu74 and Fe52, which by the way may produce a complex oxyhydroxides mixture (copper–zinc hydroxide and iron–zinc hydroxide). Here we concluded that removal efficiency was not a function of the electrode purity, but depends mainly on the structure of the molecule. Satisfactory photocatalytic removal of the dye CBWB has also been reported (Poulios and Tsachpinis, 1999) after 20 min radiation from a  $40 \text{ mg l}^{-1}$  dye solution. Vat, reactive and direct dyes have been removed with 87–100% efficiency in terms of color removal (Jia et al., 1999) by using an electrode made of carbon fiber and a piece of iron after 60 min treatment applying a high potential of 25 V. Removal of reactive dyes from real dyeing wastewater (Vlyssides et al., 2000) reached 77% by electrooxidation using Ti/Pt as anode, but unfortunately the potential value was not reported. In that work we can access to the energy consumption data reported as  $22 \text{ kWh kg}^{-1}$  organic load after 15 min oxidation. Treatment efficiency quoted in Table 3 in terms of  $t_{50\%}$  could have economical importance, as well as the potential magnitude, when the energy consumption of the process is considered. Results obtained with iron and aluminium electrodes (Kobya et al., 2003) showed that, as in our case, aluminium was inferior to iron from the energy consumption and efficiency points of view.

### 3.3. Influence of pH on the system CBWB dye-Fe52 electrode

The time necessary for degradation depends mainly upon the concentration and stability of the solutes, when other factors as temperature, potential, flow and electrodes geometry and nature have been optimized. Almost all dyes are represented by molecules consisting of atomic systems with abundant  $\pi$ -electrons, which are also responsible for color. Any color change, as in the case of indicators, can be associated with the structural or electrons distribution changes that may be induced by protons, according to the scheme for a general dye moiety:



Although it was reported (Jia et al., 1999) that the effect of pH was not significant in the treatment of dyeing wastewater, protonation and deprotonation may modify the affinity of the dye for the electrochemically generated ionic species. So we explored the performance of the Fe52 electrode in the color removal of the dye CBWB at pH 7 as described above and additionally at pH 5.5. When  $C_t/C_0$  vs.  $t$  graphs as those depicted in Figs. 1 and 2 are plotted in logarithmic scale, a linear dependence provides direct kinetic information. This would indicate a first order kinetics reaction and the higher the absolute slope value, the higher the rate constant as it can be appreciated in Fig. 3. Furthermore, quantitative evaluation of the slope by the common linearization procedures yielded the rate constant values listed in Table 2 for Fe52 at pH 5.5 and 7. When the process takes place in the presence of oxygen in a one-compartment cell at  $-2.5$  V the following reactions can take place:



These reactions depend on the pH of the solution and on the potential and it is known that the half-reactions may modify the pH in the vicinity of the electrode. The

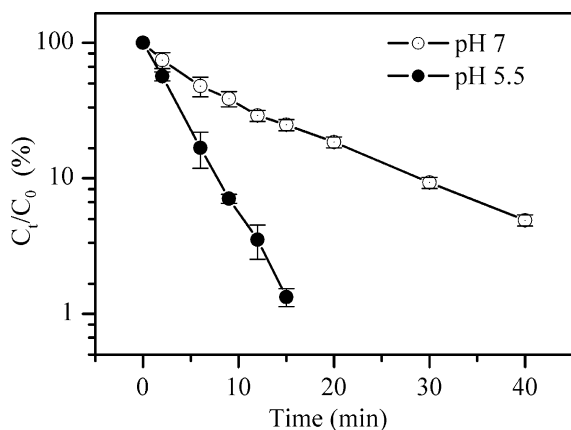
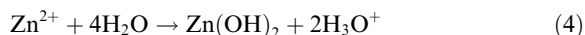
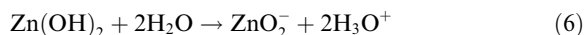
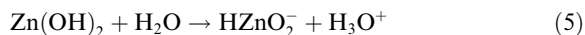


Fig. 3. Linear dependence of the concentration with time for the first order kinetics electrolysis reaction of Cibacron WB at different pH  $\pm 0.1$  values at the Fe52 electrode ( $-2.5$  V) with flow at  $3 \text{ ml min}^{-1}$ .

Pourbaix diagrams overlaying the redox and acid–base chemistry of metals showed that at the potential and pH conditions of our experiments the following species of iron and zinc could be present at pH 5.5 and 7:  $\text{Fe}_{(\text{s})}$  (Coleman, 2003),  $\text{Zn}_{(\text{s})}$ ,  $\text{Zn}_{(\text{aq})}^{2+}$  and  $\text{Zn}(\text{OH})_2$  ( $\text{s, amorphous}$ ) (Rotinyan et al., 1981). These species may appear in negligible amounts when the electrodes remained at open circuit potential for about 5–10 min before electrolysis. For the CBWB dye studied at  $-2.5$  V on the Fe52 electrode at pH values of 5.5 and 7.0, it was observed that the rate constant (Table 2) was four times greater at pH 5.5 than at pH 7.0. When pH was 5.5 the dye presents the tautomeric forms (1b + 1c) depicted in Eq. (1), while  $\text{H}_2$  was produced abundantly according to Eq. (3) and the single ionic species was  $\text{Zn}^{2+}$  (Rotinyan et al., 1981) coming from the Zn component of the Fe52 electrode. Reduction of the non-adsorbed dye as a free positive species occurred readily by consumption of  $\text{H}_2$  since the reaction:



was thermodynamically impossible ( $\Delta G^{298} = +1.5 \text{ kJ mol}^{-1}$ ) at pH 5.5. We calculated the Gibbs free energy variation of  $\text{Zn}(\text{OH})_2$  of Eq. (4) and of the following zinc hydroxide and zincate for the pH value of 7, which according to Rotinyan et al. (1981) can be formed:

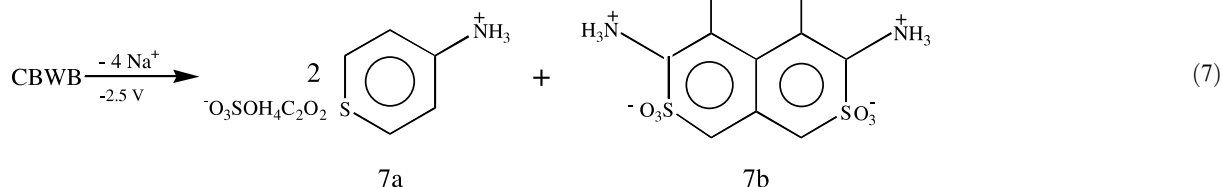


The species generated at pH 7 by reactions (4)–(6) can be arranged according to their thermodynamically favorable formation:  $\text{ZnO}_2^{2-}$  ( $\Delta G^{298} = -88.2 \text{ kJ mol}^{-1}$ ) >  $\text{HZnO}_2^-$  ( $\Delta G^{298} = -54.5 \text{ kJ mol}^{-1}$ ) >  $\text{Zn}(\text{OH})_2$  ( $\Delta G^{298} = -15.6 \text{ kJ mol}^{-1}$ ). The electrostatic interactions between the species  $\text{ZnO}_2^{2-}$  and  $\text{HZnO}_2^-$  formed on the electrode surface and the positively charged dye would be stronger in comparison with the dispersive interaction between the uncharged surface species  $\text{Zn}(\text{OH})_2$  and the dye in equilibrium. Facing this situation it can be postulated that at  $-2.5$  V a faster dye reduction process at pH 5.5 took place as a result of the absence of rising interactions between the dye and the zinc species. A slower reaction and the fact that by similar COD removal (see Table 3) the decolorization of the dye after 40 min electrolysis was less (see Fig. 3) at pH 7 than at pH 5.5

could be explained by considering the complexity of the interactions in the electrode surface.

### 3.4. Electroreduction products of the system CBWB dye-Fe52 electrode

To demonstrate the formation of degradation or reduction products during monitoring of the electrochemical treatment, Fig. 4 shows chromatograms of the initial solution and after electrolysis of the sulfoazo CBWB dye using the electrode Fe52. After 15 min electroreduction the dye peak appearing at retention time 15 min was no more observed at detection wavelength 220 nm. The main reason for not selecting the dye maximum absorbance wavelength in this part of the study was the fact that decomposition components presenting absorbance bands in the UV spectral region could be monitored. As it can be appreciated in Fig. 4, there are two new components (7a and 7b) in the solution, which presented smaller retention times than the dye molecule. This indicates the presence of compounds exhibiting less hydrophobicity (regarding the reverse stationary phase) and correspondingly lower carbon atom number than the original dye molecule. Since chemical reduction of the azo linkage commonly results in the formation of lower molecular weight aromatic amine entities and produces the parallel elimination of color in the reduced solutions of the dyes, the following intermediate reaction can be postulated for the CBWB dye:



Here the (7a) and (7b) molecule fragments probably correspond to the two peaks observed in Fig. 4 after 15 min electrolysis, which disappeared from the batch solution at the end of the procedure.

The curves in Fig. 3 together with the constant rates listed in Table 2 demonstrated that the process occurred with distinct rate at different pH, but the most interesting result was the absence of precipitate formed in the cell bottom, when electrolysis was carried out in phosphates buffer at pH 5.5. In experiments performed in phosphates buffer at pH 7, we observed formation of white-bluish sludge at the cell. Due to its color, the

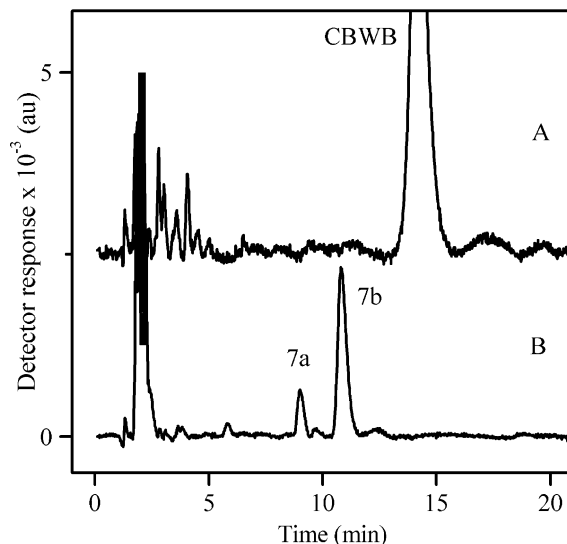


Fig. 4. Chromatograms of the CBWB dye solutions after 15 min electrolysis (B) under dynamic regime with flow at  $3 \text{ ml min}^{-1}$  in comparison with the solution before electrolysis (A). Working electrode Fe52. Column OCTYL, flow rate  $0.8 \text{ ml min}^{-1}$ , mobile phase: (20:80) aqueous phosphate buffer, pH 5-methanol (2.5 min) and linear gradient buffer-methanol (20:80) to (50:50). Temperature  $25^\circ \text{C}$ . Detection wavelength 220 nm.

white-bluish precipitate could contain some blue dye. However the IR spectrum shown in Fig. 5A (continuous line) did not correspond to the dye IR spectrum

although the observed bands at  $1607 \text{ cm}^{-1}$  and  $3051 \text{ cm}^{-1}$  could be assigned to the azo ( $1630 \text{ cm}^{-1}$ ) and aromatic ( $3030\text{--}3080 \text{ cm}^{-1}$ ) groups. This spectrum could be related then with two or more solids in mixture producing overlapping bands. In order to discriminate the adsorption or deposition of the blue dye onto a potentially white precipitate, the sludge was leached thoroughly in water and in methanol. The leachate did not present the absorption band of the dye as presented in Fig. 5B. The feasibility of metals to build complexes with dyes (Baughman, 2001) and azo-compounds in general (Wang et al., 2000) is well known. Since sulfonate

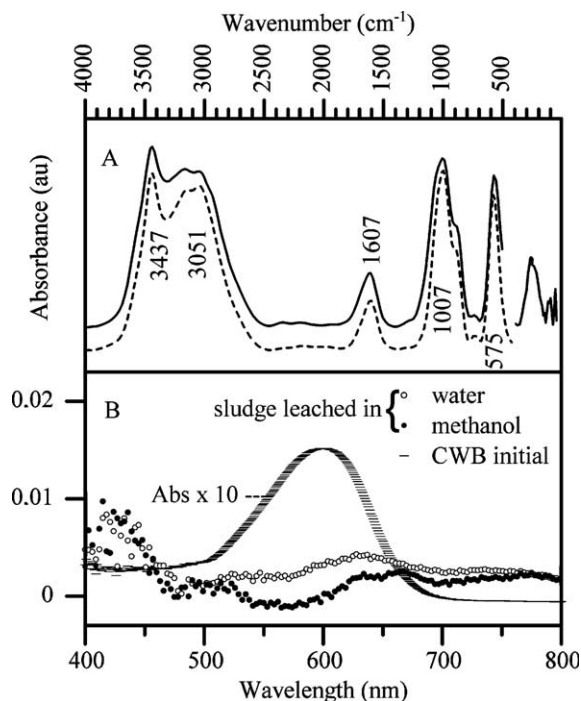


Fig. 5. FTIR spectra (A) of the electrolysis sludge (continuous line) and of the precipitate in absence of the dye CBWB (dotted line) and VIS spectra (B) of the dye solution of the leachate.

complexes of Orange G have been reported by Bandara et al. (1999) during the adsorption of the dye on Fe, Ti and Al oxides; the idea of a sludge coming from a complex formed between the dye and the metal of the electrode seemed plausible. A blank electrolysis experiment (phosphates buffer at pH 7 in absence of dye) demonstrated contrary to our expectations, that no dye was contained in the sludge since the spectra of the precipitate obtained with dye (continuous line) and without dye (dotted line) in Fig. 5A were identical. The spectra were very similar to those obtained for metal phosphates (Mustafa et al., 1999; Dinamani and Kamath, 2001), whereby the bands in Fig. 5A at 575 and 1007  $\text{cm}^{-1}$  can be assigned to P–O stretching and bending vibrations, respectively; and at 1607 and 3000–3500  $\text{cm}^{-1}$  to O–H stretching and bending, respectively indicating that the metal phosphate is hydrated. X-ray characterization of the sludge obtained with dye and without dye yielded identical patterns and the following results:  $92 \pm 2\%$   $\text{Fe}_3(\text{PO}_4)_2 \cdot 8\text{H}_2\text{O}$  (*vivianite*) +  $8 \pm 2\%$   $\text{Fe}(\text{PO}_4) \cdot 2\text{H}_2\text{O}$  (*fosfoserite*). Fig. 6 shows the diffraction pattern obtained in presence of dye, where 28 peaks corresponding to ferrous phosphate (PDF 3-70) and 6 peaks of the ferric phosphate (PDF 15-390) could be identified. No peaks corresponding to zinc or nickel phosphates could be found. Organic ligands, if present, could only be amorphous or in amounts less than 1%.

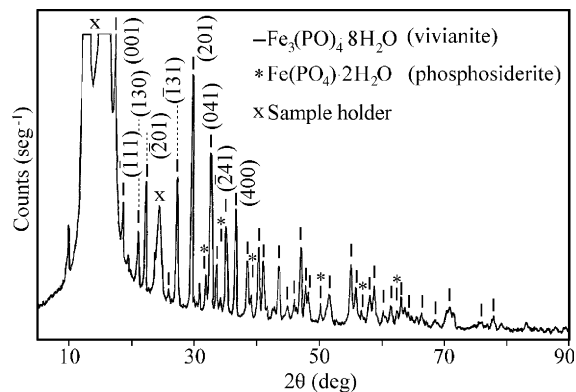


Fig. 6. X-ray diffraction pattern of the sludge obtained after electrolysis of the CBWB dye performed with the Fe52 electrode at  $-2.5$  V with flow at  $3 \text{ ml min}^{-1}$  and pH 7 in phosphate buffer.

The phosphates obtained here are interesting byproducts from the point of view of their synthesis, since metal phosphates are usually obtained by precipitation, melting or sol-gel methods (Scaccia et al., 2003) and as demonstrated for cobalt phosphate (Dinamani and Kamath, 2001) the product obtained via electrochemical reduction differed from the phase obtained by precipitation.

The formation of the sludge, which amounted 0.9% of the electrode weight, can be explained as follows. The corrosion potential with respect to time in the solution was monitored for each system in order to study the relative surface reactivity. A decrease from  $-800$  to  $-1000$  mV was observed during the first five minutes and then stabilized indicating iron corrosion leading to iron dissolution under open-circuit conditions. In this case a  $\text{Fe}_2\text{O}_3$  oxide film can be expected. Since during electrolysis hydrogen was produced, ferric iron reduced to ferrous iron and we can presume that they reacted with the phosphate ions of the buffer solution and precipitated as ferrous (92%) and ferric (8%) phosphates as described above. The Al99 and the Cu74 electrodes did not produce precipitate. Their corrosion potentials shifted relatively quickly to a more noble values of  $-534$  and  $-100$  mV, respectively and remained steady at that value for the duration of the experiment indicating stable  $\text{Al}_2\text{O}_3$  and  $\text{CuO}$  film formation.

Electrolysis was carried out also at pH 5.5 without phosphate buffer and as it was expected we did not observe sludge formation during electroreduction of the dye CWBW on the Fe52 electrode. In presence of phosphates at pH 5.5 the reaction occurred faster as discussed above and did not produce precipitate. This has the advantage of minimizing the amount of total dispersed solids, which is one of the specific objectives established, by textile mills. Since in our case solubility of the hydroxides formed on the electrode surface par-



tially controls the solubility of the electrode metal in a given medium and hence the precipitate formation, we calculated the concentrations of the total hydroxide species present in the studied systems as a function of pH by using solubility product values and compared the domains of the curves (not shown here) with the solubility of the metal phosphates. The relative position of the ferric hydroxide and ferric phosphate curves could not explain both the dissolution of the precipitate at pH 5.5 and the precipitation of the sludge at pH 7.

#### 4. Conclusions

The results obtained confirm the applicability of non-conventional electrodes and of HPLC to follow color removal and formation of products. Kinetics of the degradation of SLY dye on a diamond electrode demonstrated the benefit of a dynamic regime with flow. The study of the effect of the applied potential indicated that a potential of  $-2.0$  V is effective under these conditions for the removal of the dye CBWB. The efficiency of the studied electrodes for removal of the dye CBWB in terms of COD obeyed the series:  $Al99 < Cu74 \approx Fe52$ . Degradation of the dye CBWB occurred four times faster at pH 5.5 than at pH 7, where additionally a ferric-ferrous phosphate sludge was obtained.

#### Acknowledgements

M.C.R. thanks CONACyT for a scholarship grant (130 528). The authors are grateful to P. Morgenstern (UFZ—Centre for Environmental Research, Leipzig, Germany), and S. Bernès (UAP) for the XRFs and XRD measurements, respectively and thank M. González-Perea (UAP) for his help in the experiments.

#### References

- American Society for Testing and Materials (ASTM), 2003. D1252-00 Standard Test Methods for Chemical Oxygen Demand (Dichromate Oxygen Demand) of Water.
- Bandara, J., Mielczarski, J.A., Kiwi, J., 1999. Molecular mechanism of surface recognition. Azo dyes degradation on Fe, Ti, and Al oxides through metal sulfonate complexes. *Langmuir* 15, 7670–7679.
- Baughman, G.L., 2001. Fate of copper-complexed dyes during biological waste treatment III. *Dyes Pigments* 48, 179–186.
- Coleman, W.F., 2003. Pourbaix diagrams and reactions in aqueous solution. Available from <<http://www.wellesley.edu/Chemistry/chem120/pour.html>>.
- Dávila-Jiménez, M.M., Elizalde-González, M.P., Gutiérrez-González, A., Peláez-Cid, A.A., 2000. Electrochemical treatment of textile dyes and their analysis by high performance liquid chromatography with diode array detection. *J. Chromatogr.* 889, 253–259.
- DeFazio, S.A.K., Lemley, A.T., 1999. Electrochemical treatment of acid dye systems: sodium meta-bisulphite addition to the Andco system. *J. Environ. Sci. Health, Part A* 34, 217–240.
- Delée, W., O'Neill, C., Hawkes, F.R., Pinheiro, H.M., 1998. Anaerobic treatment of textile effluents: A review. *J. Chem. Technol. Biotechnol.* 73, 323–335.
- Dinamani, M., Kamath, P.V., 2001. Electrochemical synthesis of metal phosphates by cathodic reduction. *Mater. Res. Bull.* 36, 2043–2050.
- Goheen, S.C., Durham, D.E., McCulloch, M., Heath, W.O., 1994. The degradation of organic dyes by Corona discharge. In: Eckenfelder, W.W., Bowers, A.R., Roth, J.A. (Eds.), *Chemical Oxidation*, vol. 2. Technomic Publishing Co. Inc., Lancaster, Basel, pp. 356–367.
- Gregor, K.H., 1994. Oxidative decolorization of textile waste water with advanced oxidation processes. In: Eckenfelder, W.W., Bowers, A.R., Roth, J.A. (Eds.), *Chemical Oxidation*, vol. 2. Technomic Publishing Co. Inc., Lancaster, Basel, pp. 161–169.
- Ince, N.H., 1999. “Critical” effect of hydrogen peroxide in photochemical dye degradation. *Water Res.* 33, 1080–1084.
- Jia, J., Yang, J., Liao, J., Wang, W., Wang, Z., 1999. Treatment of dyeing wastewater with ACF electrodes. *Water Res.* 33, 881–884.
- Kobyas, M., Can, O.T., Bayramoglu, M., 2003. Treatment of textile wastewaters by electrocoagulation using iron and aluminium electrodes. *J. Hazard. Mater.* 100, 163–178.
- McClung, S.M., Lemley, A.T., 1994. Electrochemical treatment and HPLC analysis of wastewater containing acid dyes. *Text. Chem. & Colorist* 26, 17–22.
- Morais, L.C., Freitas, O.M., Gonçalves, E.P., Vasconcelos, L.T., González Beça, C.G., 1999. Reactive dyes removal from wastewaters by adsorption on Eucalyptus bark: variables that define the process. *Water Res.* 33, 979–988.
- Mustafa, S., Naeem, A., Murtaza, S., Rehana, N., Samad, H.Y., 1999. Comparative sorption properties of metal (III) phosphates. *J. Colloid Interf. Sci.* 220, 63–74.
- Poulios, I., Tsachpinis, I., 1999. Photodegradation of the textile dye Reactive black 5 in the presence of semiconducting oxides. *J. Chem. Technol. Biotechnol.* 74, 349–357.
- Powell, W.W., Michelsen, D.L., Boardman, G.D., Dietrich, A.M., Woodby, R.M., 1994. Removal of color and TOC from segregated dye discharges using ozone and Fenton's reagent. In: Eckenfelder, W.W., Bowers, A.R., Roth, J.A. (Eds.), *Chemical Oxidation*, vol. 2. Technomic Publishing Co. Inc., Lancaster, Basel, pp. 278–300.
- Rotinyan, A.L., Tikhonov, K.I., Schoschina, I.A., 1981. *Theoretical Electrochemistry*. Khimiya, Leningrad. pp. 174–176.
- Scaccia, S., Carewska, M., Di Bartolomeo, A., Prosini, P.P., 2003. Thermoanalytical investigation of nanocrystalline iron (II) phosphate obtained by spontaneous precipitation from aqueous solution. *Thermochim. Acta* 397, 135–141.
- Sedahmed, G.H., Farag, H.A., Zatout, A.A., Katkout, F.A., 1986. Mass transfer characteristics of gas-sparged fixed-bed electrodes composed of stacks of vertical screens. *J. Appl. Electrochem.* 16, 374–378.

- Sheng, H., Peng, Ch.F., 1994. Treatment of textile wastewater by electrochemical method. *Water Res.* 28, 277–282.
- Shen, Z., Wang, W., Jia, J., Ye, J., Feng, X., Peng, A., 2001. Degradation of dye solution by an activated carbon fiber electrode electrolysis system. *J. Hazard. Mater. B* 84, 107–116.
- Vandevivere, P.C., Bianchi, R., Verstraete, W., 1998. Treatment and reuse of wastewater from the textile wet-processing industry: review of emerging technologies. *J. Chem. Technol. Biotechnol.* 72, 289–302.
- Van Hege, K., Verhaege, M., Verstraete, W., 2002. Indirect electrochemical oxidation of reverse osmosis membrane concentrates at boron-doped diamond electrodes. *Electrochem. Commun.* 4, 296–300.
- Vlyssides, A.G., Papaioannou, D., Loizidou, M., Karlis, P.K., Zorpas, A.A., 2000. Testing an electrochemical method for treatment of textile wastewater. *Waste Manage.* 20, 569–574.
- Wang, S., Shen, S., Xu, H., 2000. Synthesis, spectroscopic and thermal properties of azo metal chelate dyes. *Dyes Pigments* 22, 195–198.
- Wilcock, A.E., Brewster, M., Peck, G., 1996. Use of electrochemical technology to remove color and other contaminants from textile effluents. In: Reife, A., Freeman, H.S. (Eds.), *Environmental Chemistry of Dyes and Pigments*. John Wiley & Sons, Inc., New York, Chichester, Brisbane, Toronto, Singapore, pp. 61–74.
- Xiong, Ya., Strunk, P.J., Xia, H., Zhu, X., Karlsson, H.T., 2001. Treatment of dye wastewater acid orange II using a cell with three-phase three-dimensional electrode. *Water Res.* 35, 4226–4230.
- Yang, C.-H., Lee, C.-C., Wen, T.-C., 2000. Hypochlorite generation on Ru–Pt binary oxide for treatment of dye wastewater. *J. Appl. Electrochem.* 30, 1043–1051.